Desalination and Water Treatment
www.deswater.com

doi:10.5004/dwt.2018.22916

124 (2018) 53–61
August

Investigation of organic compounds on the performance of membrane capacitive deionization: desalination rate, energy consumption and its mechanisms

Lin Chen[a,b,*], Chengyi Wang[a,b], Shanshan Liu[a,b], Liang Zhu[a,b]

[a]*Key Laboratory of Integrated Regulation and Resources Development of Shallow Lakes, Hohai University, Nanjing 210098, China, email: chen_lin@hhu.edu.cn (L. Chen)*
[b]*College of Environment, Hohai University, Nanjing 210098, China*

Received 13 November 2017; Accepted 4 August 2018

ABSTRACT

Attention in desalination using membrane capacitive deionization (MCDI) has led to the realization that organic substances may cause undesirable attachment onto membrane and could affect the MCDI desalination performance. Bovine serum albumin (BSA) was used as a model foulant and its effects on the desalination rate and membrane properties were studied during long-term operation. The desalination rate was found to be relatively stable (48.05%) when the feed solution contained NaCl only, while the rate significantly decreased to 4.3% when 100 mg/L BSA was present in the feed water. Energy consumption increased obviously due to the additional energy consumed by BSA and the increment became more significant with BSA concentration increasing. The phenomenon was further analyzed using different characterization methods and it was found that the changes in membrane properties and surface structure caused by the initial aggregate deposition onto membrane surfaces followed by the chemical attachment of native protein molecules onto these aggregates were the main reasons for the decline in the desalination rate. Eventually, a series of cleaning steps were adopted to select the most effective method for ion exchange membrane in MCDI process. These findings would offer deeper insights into the effect of organic substance on MCDI performance, which was expected to provide a theoretical basis for further application.

Keywords: Membrane capacitive deionization; Membrane properties; Desalination rate; Energy consumption; Organic substance

1. Introduction

With the rapid development of urbanization and industrialization, the global water shortage has become more serious and the demands for fresh water resources are more urgent [1]. Many regions suffer from brackish ground water and this situation has affected billions of people around the world [2]. To alleviate this dilemma, various desalination technologies including reverse osmosis (RO), electrodialysis (ED) and membrane distillation (MD) have been gradually applied in the water desalination. Although these methods are currently effective in water desalination, some shortcomings such as high energy consumption and operation cost limit their further wide-application [3]. Hence, it becomes urgent to explore a new method of water desalination which can overcome these limitations. Capacitive deionization (CDI) basically including the absorption and desorption process has aroused wide concerns in recent years as a low cost, energy saving and environmental friendly electrochemical desalination technology [4]. In its adsorption process, ions in the inlet stream are adsorbed onto the electrodes to purify water as the voltage is applied. When the system is switched to the desorption process, the adsorbed ions are released back into the waste stream by reversing voltage [5] and thus the electrode is regenerated and recovered its adsorption capacity [6]. Membrane capacitive deionization (MCDI), a modification of CDI by combining with ion-exchange membranes, performs on the basis of the same working principle [7]. In MCDI, ion exchange membranes are displaced in front of the electrodes to pre-

*Corresponding author.

vent co-ions effect,which would significantly enhance the desalting efficiency and increase charge efficiency [8].

Regarding its great performance and improvement, MCDI process has been investigated in several aspects including the evaluation of its economic viability and assessment of newly developed or synthesized electrodes [9]. However, few studies have focused on the effect of organic matters on desalination performance. As far as we known, an inevitable problem in membrane application is the undesirable attachment of organic substances onto membrane surface and this fouling phenomenon has raised great attentions [10,11]. Membrane fouling may markedly reduce the desalination rate, decrease product quality and consequently increase the operating costs. Lee et al. [12] reported that natural organic matter (NOM) would be absorbed onto membrane and deteriorate membrane properties as well desalination performance during electrodialysis. Naidu et al. [13] investigated the membrane fouling in direct contact membrane distillation (DCMD) using synthetic solution of bovine serum albumin (BSA), and the results showed that more significant deposits of BSA on membrane surface resulted in significant pore penetration. It was found by Tanaka et al. [14] that aromatic organic substances would cause severe organic fouling on anion exchange membrane with divinylbenzene and chloromethylstyrene base matrix due to affinity interaction between the membrane matrix and aromatic substances. However, fouling has not been publicly addressed during long-term operation in MCDI and it is necessary to investigate the effect of organic matters on the treatment efficiency of MCDI, especially the performance of ion exchange membrane, which has not been discussed previously.

The aim of this work was to investigate the presence of organic matter on the membrane properties and desalination performance during 15 d operation in MCDI process systemically. The effects of organic matter were characterized by the analysis of membrane properties (ion exchange capacity, water content, electrical resistance and transport number), desalination performance, energy consumption, and membrane morphology. Additionally, a series of cleaning steps were adopted to study effective methods for ion exchange membrane in MCDI process.

2. Experimental sections

2.1. MCDI set-up

The structure of MCDI unit in this study is displayed in Fig. 1. The carbon fiber (Jiangsu branch Carbon Fiber Co., Ltd, KJF-1300) with 0.025 m^2 surface area acted as electrodes to absorb ions in the feed solution. The ion exchange membranes (Hangzhou Greenhe Environment Co., Ltd, China) with high permselectivity were attached onto the carbon electrodes and separated by a spacer (thickness = 1 mm) to form a flow channel and prevent electrode short-circuit. After assembly, all layers in the stack were compressed and placed in the plexiglass with the dimension of 25×20 cm^2. To prevent short-circuiting, two holes with 1 cm were drilled on each side of plexiglass plate acting as inlet and outlet. The whole system (as shown in Fig. 2) consisted of influent tank, conductivity monitor (Shijiazhuang Ji Shen Electronic Technology Co., Ltd, EC-1800),

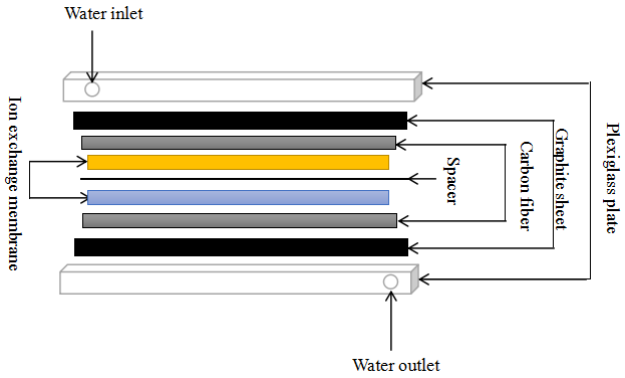

Fig. 1. Schematic diagram of MCDI unit.

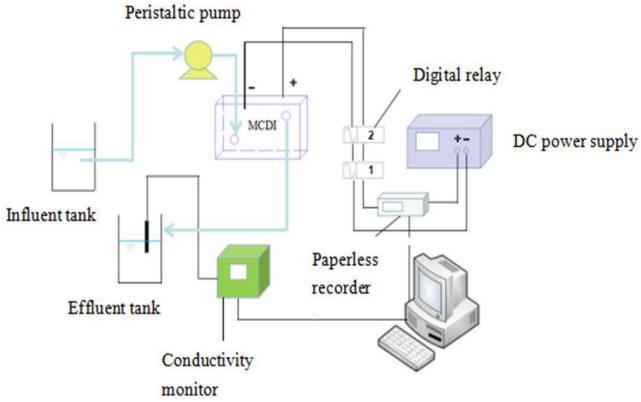

Fig. 2. Schematic illustration of MCDI system.

digital relay (Qin Yang Electric Co., Ltd, DH48S-S), peristaltic pump (YZ II 15, Longer Precision Pump Co., Ltd, China), paperless recorder (THTZ408R, Penghe Electronics Co., Ltd, China), effluent tank and potentiostat (IT6720, Itech Co., Ltd, China).

2.2. Desalination experiment

For each experiment, feed solution flowed into the MCDI desalination component which was driven by the peristaltic pump with a constant rate of 5 mL/min. Potentiostat loaded forward voltage at both ends of the component and the charging voltage was set at 1.2 V to conduct desalination. A complete MCDI operation cycle included a 55 min absorption step and a 40 min generation step, in which regeneration was carried out by reversing the voltage under the control of digital relay. The corresponding electrical current across the electrodes was measured automatically by paperless recorder every 5 s.

Four different feed solutions were prepared to investigate the effect of the presence of BSA on desalination performance, as shown in Table 1. The chemicals included NaCl and BSA (98% purity, Sinopharm Chemical Reagent Co., Ltd.), which were dissolved in deionized water (DI water). The conductivity of the effluent from the MCDI cell was measured using a conductivity meter and then converted to the actual concentration. Additionally, solution F5 only con-

Table 1
Water quality of feed solutions

Parameters	Feed solutions				
	F1	F2	F3	F4	F5
NaCl (mg/L)	140	140	140	140	0
BSA (mg/L)	0	5	40	100	100
Conductivity (μS/cm)	400	399	410	406	24

taining BSA was prepared and its concentration was measured over time to investigate whether BSA could degrade naturally in solution.

2.3. Analysis methods

The desalination rate of MCDI (η) was calculated according to Eq. (1):

$$\eta(\%) = \frac{C_o - C_a}{C_o} \times 100\% \quad (1)$$

where C_o and C_a (mg/L) represent the initial concentration of salt solution and the average concentration of effluent solution, respectively.

The specific energy consumption was an important parameter to evaluate the economic performance of MCDI, which was calculated by the ratio of the electric energy consumed in the desalting process to absorb salt.

$$W = \frac{E}{Q_w} \quad (2)$$

where W is the specific energy consumption (W·h/g), E is the energy consumed in the desalination process (W·h), and Q_w is the absorbed salts during desalination (g).

The current efficiency was specifically calculated as Eq. (3):

$$\eta(\%) = \frac{(C_i - C_f) \times V_f \times F}{\int Idt} \times 100 \quad (3)$$

where C_i and C_f represent NaCl concentration in feed water and the effluent (mol/L), respectively. V_f is the effluent volume, F is Faraday constant, 96500 C/mol, I is the current flowing through the MCDI at the adsorption stage (A), and t is desalination time (s).

2.4. Membrane characterization

The physical and chemical properties of the anion exchange membrane were analyzed in terms of electrical resistance, transport number, water content and ion exchange capacity. Each sample was measured for 3 times to avoid the accidental error.

Membrane electrical conductivity could be obtained via the membrane conductance using the clip-cell with two platinum electrodes, and calculated as follows [15]:

$$R_m = \frac{1}{G_m} = \frac{1}{G_{m+s}} - \frac{1}{G_s} = R_{m+s} - R_s \quad (4)$$

where R_m is the membrane electric resistance, R_s is the resistance of the reference solution, R_{m+s} is the resistance of membrane with reference solution, G_m, G_{m+s} and G_s represent the conductance of the membrane, reference solution and membrane with reference solution, respectively.

Determination of transport number (t_+) was calculated according to the potential difference produced by ion migration [16]. Two feed solutions with different NaCl concentrations were prepared to create the concentration gradient, and the potential difference near the membrane solution interfaces was monitored via the Luggin capillary and Ag/AgCl electrodes. The Na^+ transport (1:1 electrolyte) can be obtained from:

$$E = (2t_+ - 1)\frac{RT}{F}\ln\frac{C_1}{C_2} \quad (5)$$

where t_+ is the transport number, E is the potential difference (V), R is the molar gas constant (J/mol·K), T is the temperature (°C), C_1 and C_2 are the NaCl concentrations ($C_1 > C_2$).

For ion exchange capacity, the membranes were soaked in 0.1 N NaOH solution to exchange the counter-ion from Cl^- to OH^- [17], and then the concentration of exchanged OH^- was estimated by the amount of 0.01 N HCl consumed using the automatic titrator with an end-point of pH 7.

$$IEC = \frac{V_{Sol} C_{OH^-}}{W_{dry}} \quad (6)$$

where W_{dry} is the weight of membrane under dry condition and C_{OH^-} is the concentration of OH^-.

For water content, membrane samples which were equilibrated in water at a given temperature (60°C) were weighed in wet form, and then samples were dried in vacuum oven at elevated temperature until a constant weight was attained [18].

$$wt\% = \frac{W_{wet} - W_{dry}}{W_{dry}} \times 100\% \quad (7)$$

where W_{wet} is the weight of wet membrane, and W_{dry} is the weight of dry membrane.

To determine the amount of BSA attached on the membrane surface, the amounts of protein on the membrane surface was determined using the bicinchoninic acid method [19].

The morphology of the fresh membrane and the fouling layer on the membrane surface was evaluated by scanning electron microscope (SEM) (SIPRA55, ZEISS, Germany). Except for the fresh membrane, other samples were taken on day 15 and dried before mounting on stubs and gold sputtering for SEM detection.

3. Results and discussions

3.1. Effects of BSA concentration on desalination rate

Four independent experiments were conducted to investigate the effect of feed solutions with different BSA concentrations on MCDI performance, as shown in Fig. 3. It was observed that, when the MCDI cell was fed with solution F1, containing NaCl only, the desalination rate

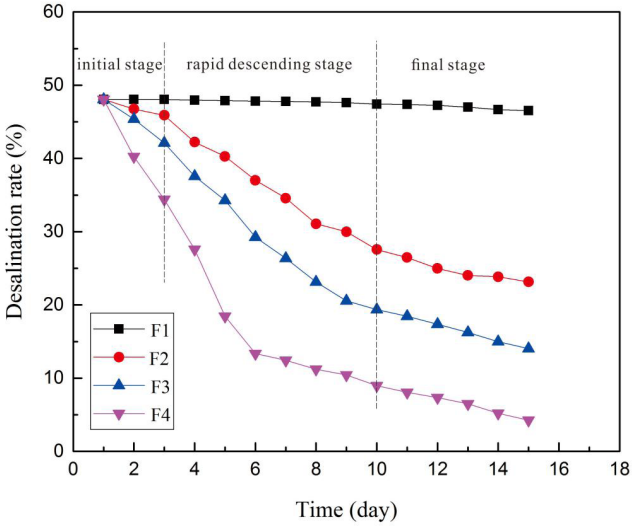

Fig. 3. Variations of desalination rate for the four different feed solutions.

Table 2
Initial concentration of BSA in the feed solution and absorption amount of BSA on membrane surface

	F1	F2	F3	F4	F5
Initial concentration of BSA (mg/L)	0	5	40	100	100
Absorption amount of BSA (μg/cm^2)	0	0.45	5.12	14.85	0

remained 48.1% and no obvious reduction in desalination rate occurred during the 15 d operation. Comparatively, the addition of 5 mg/L BSA resulted in an obvious drop in desalination rate which declined from 47.9% to 23.1% within 15 d for F2, indicating that the presence of BSA had an adverse effect on the desalination performance. Regarding F3 and F4 containing higher BSA concentrations, more significant reduction in desalination rate was observed and the whole process could be divided into three stages including the initial stage, rapid descending stage and the final (stable) stage.

In the initial stage, the desalination rate of F3 and F4 presented a slight decreasing tendency to 43.8% and 40.2% within 4 d, respectively. Generally, BSA in water solution usually existed in the form of aggregates and the average particle size was about 300 nm [20]. The larger size of BSA aggregates contributed to the relatively slower molecule mobility in the solution, naturally resulting in a milder deposition behavior. Thus, a slight downward trend was observed initially. In the rapid descending period, the desalination rate of F3 and F4 showed further downward trend and the value significantly decreased to 20.6% and 12.1% on day 12, respectively. BSA aggregates were facile to be adsorbed onto membrane surface for their hydrophobic or amphoteric character [21], hence the membrane surface was gradually covered and fouled by BSA aggregates with the extension of operation time. These attachments after long-term accumulation were stable with strong bonds, which could was considered to be hardly broken under the electrical field and desorbed by reversing the applied voltage. As a result, a rapid decline of desalination rate was predictable. The possible reason for the tendency of final stage was attributed to the adsorption equilibrium of BSA aggregates on the ion-exchange membrane surface. In other words, BSA was adsorbed onto the ion-exchange membranes and equilibrated after a period of time, and later BSA aggregates would not further affect membrane significantly [22]. Hence, the rates for F3 and F4 slowly decreased to 14% and 4.3% on day 15, respectively.

The absorption amount of BSA on the membrane surface was also analyzed after each experiment. For F2, only small BSA aggregates was absorbed onto the membrane surface with the concentration of 0.45 μg/cm^2. With respect to F3 and F4, an obvious increment of BSA deposition with 5.12 and 14.85 μg/cm^2 was obtained on the membrane surface, nearly dozen times increment of the deposition compared to F2. The results confirmed that BSA molecules were absorbed onto the membrane surface under the electrical field and the initial concentration of BSA had an important influence on the absorption amount. Additionally, solution F5 kept static without any treatment and BSA concentration was measured after 15 d. It was found that there was no decrement occurred in BSA concentration in F5, indicating that BSA could not degrade naturally.

Conclusively, it was reasonable to infer that the presence of BSA in the feed solution would deposit on membrane surface and exhibit an adverse effect on desalination performance in MCDI. BSA molecules tended to be aggregated in solution by intermolecular disulfide bonds [23], and its size can even reach up to micron level. Under the action of electric field, ions (Na^+, Cl^-) and BSA aggregates moved towards the membrane surface, while it was difficult for BSA aggregates to pass through the membrane pores because of the small pore size for ion exchange membrane (1–3 nm). As a result, seldom BSA molecules properly entered into the membrane pore resulting in the blockage of the membrane pores, while most of the BSA aggregates were intercepted and gradually accumulated onto the membrane surface, leading to the formation of fouling layer. Furthermore, the feed viscosity also increased with the increment of BSA concentration, further aggravating the membrane fouling and restraining the trans-membrane migration of Cl^- and Na^+ ions. Therefore, the desalination performance was deteriorated severely due to membrane fouling with the presence of BSA, especially at higher concentration.

3.2. Analysis of conductivity variation

Fig. 4 shows the conductivity variations for the four cells on day 1, 5, 10 and 15, respectively. The feed solution with an initial NaCl concentration of 140 mg/L exhibited a conductivity value of about 400 μS/cm and it was observed that the addition of BSA had no effect on initial conductivity value. For a typical working cycle in F1, the conductivity decreased sharply from 400 to 221 μS/cm at the beginning due to the migration of ions from the solution to electrode and then kept relatively steady before reaching minimum value. At the beginning of the absorption process, a large number of adsorption sites on electrode was available for ion absorption and therefore the absorption rate was rather

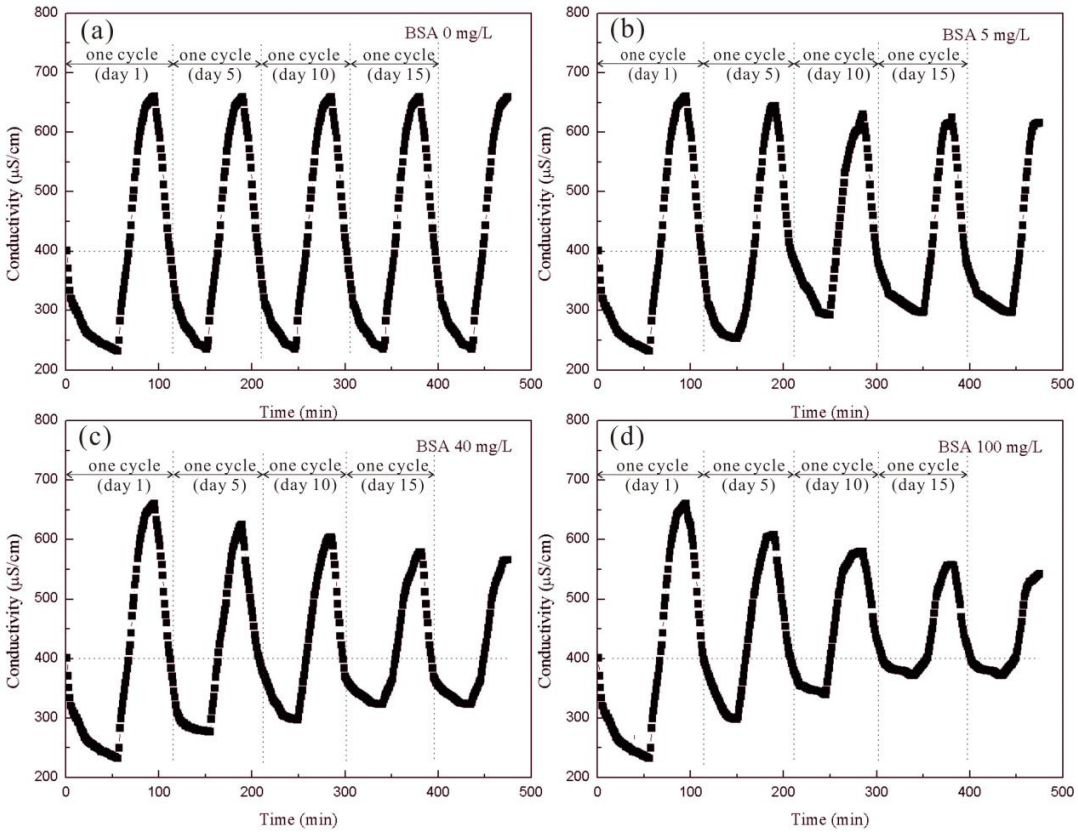

Fig. 4. Variations of cyclic conductivity on day 1, 5, 10 and 15 (a) BSA concentration 0 mg/L, (b) BSA concentration 5 mg/L, (c) BSA concentration 40 mg/L, (d) BSA concentration 100 mg/L.

faster resulting in a rapid decrement in conductivity. As the adsorption sites were gradually occupied, the competitive absorption was inevitable and the subsequent ions were electrostatically repulsive by the previously adsorbed ions, which resulted in an increment of the adsorption resistance and decrement of the adsorption rate. When the voltage was reversed in desorption process, ions were released back into solution and thus the conductivity increased to its initial value. Additionally, for F1, the cycles during 15 d operation was reproducible indicating that no variation occurred. For F2, the conductivity decreased from 399 to 240 μS/cm in one cycle on day 1 with the conductivity reduction value of 159 μS/cm. Comparatively, the conductivity slightly dropped from 401 to 298 μS/cm with the reduction value of 103 μS/cm in one cycle during the absorption process on day 5, and this variation suggested a significant decrement in salt removal. More significant discrepancy was observed in F3 and F4, and the main reason was due to the fact that the blockage of the membrane channel and the reduction of the effective membrane area inevitably resulted in deterioration of desalination performance.

The interaction between the fouling layer and ions was also an important factor causing a decrement in absorption amount. Considering the negatively charged of BSA [24], the ions in the solution were both affected by electrostatic repulsion produced by the fouling layer and electrostatic attraction produced by electrodes. In the absorption process, the electrostatic repulsion produced by fouling layer prevented the chloride ion moving towards the negative membrane, resulting in a decrement of chloride migration rate and absorption rate. Simultaneously, the amount of BSA accumulation on membrane increased and the electrostatic repulsion was strengthened with BSA concentration increasing. Hence, salt removal decreased correspondingly at adsorption equilibrium, and this variation was more significant in F3 and F4.

3.3. Characterization of membrane properties

The ion exchange membranes were named as M1, M2, M3 and M4 corresponding to the experiments using the feed solution of F1, F2, F3 and F4, and changes in the electric resistance, ion exchange capacity, transport number and water content due to membrane fouling are listed in Table 3. It could be seen that with the increment of BSA concentration, the transport numbers representing ion selectivity decreased to 0.98, 0.94, 0.83 and 0.75 for F1–F4, respectively. Similar trends were also observed for water content and ion exchange capacity, in which water content decreased to 38%, 36%, 32%, 24% and ion exchange capacity reduced to 2.5, 2.4, 2.0, 1.4 meq/g, which was related to BSA adsorption and chemical binding to the membrane surface. In addition, the electrical resistances increased to 2.6, 2.7, 2.9 and 3.2 Ω/cm^2 for M1, M2, M3 and M4, respectively. Essentially, the membrane electrical resistance was determined by pore size and transport number [15]. The narrower pore

size and lower transport number contributing to its higher resistance was consistent with the results revealed by this study. The formation of fouling layer and the lack of connectivity were responsible for higher membrane resistance. Therefore, the fouling phenomenon could also be characterized and predicted by changes in membrane properties.

Considering the small pore sizes of membrane, surface attachment should be the key factor affecting the MCDI process. Comparison of the structure of fouling layer and membrane surface was conducted using SEM. Fig. 5a illustrates that for the feed solution only containing NaCl, the membrane surface kept relatively clean with tiny amount of NaCl sticking on it (marked by red circle). For F2, the images of membrane surface in Fig. 5b displays a rough structure, in which partial membrane surface was covered with BSA aggregates and the deposition was less compact due to the relative low BSA concentration. Comparatively, obvious deposition of foulant was observed for F3 (Fig. 5c) that BSA aggregates with an approximate size of several hundred nanometers were retained on the membrane surface, forming a thin cake layer. With respect to F4, a more pronounced fouling layer was intuitively observed (Fig. 5d), in which more BSA aggregates were attached onto the membrane surface. It was clearly observed that the fouling degree was aggravated with BSA concentration increasing. Furthermore, compared to F2, the membrane surface of F3 and F4 was rather compact and complex which was attributed to physical-chemical attachment of BSA onto membrane surface.

Table 3
Characterization of the fouled membranes

Parameters	Fouled membrane			
	M1	M2	M3	M4
Electrical resistance (Ω/cm^2)	2.6	2.7	2.9	3.2
Transport number	0.98	0.94	0.86	0.75
Water content (H_2O/g)	0.38	0.36	0.32	0.24
Ion exchange capacity (meq/g)	2.5	2.4	2.0	1.4

Based on the above analysis, a composite mechanism for cake formation would be proposed to explain the fouling process. The deposition of BSA aggregates on the membrane surface in the initial stage and chemical attachment onto the previously deposited proteins at later period were mainly responsible for the surface fouling. Firstly, it was considered that BSA with high concentration had more chance to contact with membrane sites which would aggravate fouling. However, higher BSA concentration increased the chances for coagulation and formed larger particles which exhibited a slower mobility to be absorbed on the membrane surface. The mobility effect was a major factor and therefore desalination rate declined slightly in the initial stage. Additionally, the interaction between BSA and membrane was dominant this stage. BSA aggregates gradually accumulated on the membrane surface and these aggregates were subject to shear force provided by pump resulting in milder deposition. At later period, the interaction between BSA-BSA became more important with the increment attachment of BSA onto membrane. The chemical attachment was occurred via intermolecular disulfide linkage between BSA in the spacer and the protein aggregates on the membrane surface. The fouling layer served as initial sites for the continued deposition of BSA and thus aggravated the fouling process, which was consistent with the rapid descending period. Finally, the fouling layer gradually became compact and stable and later BSA just attached on the previous absorbed BSA foul-

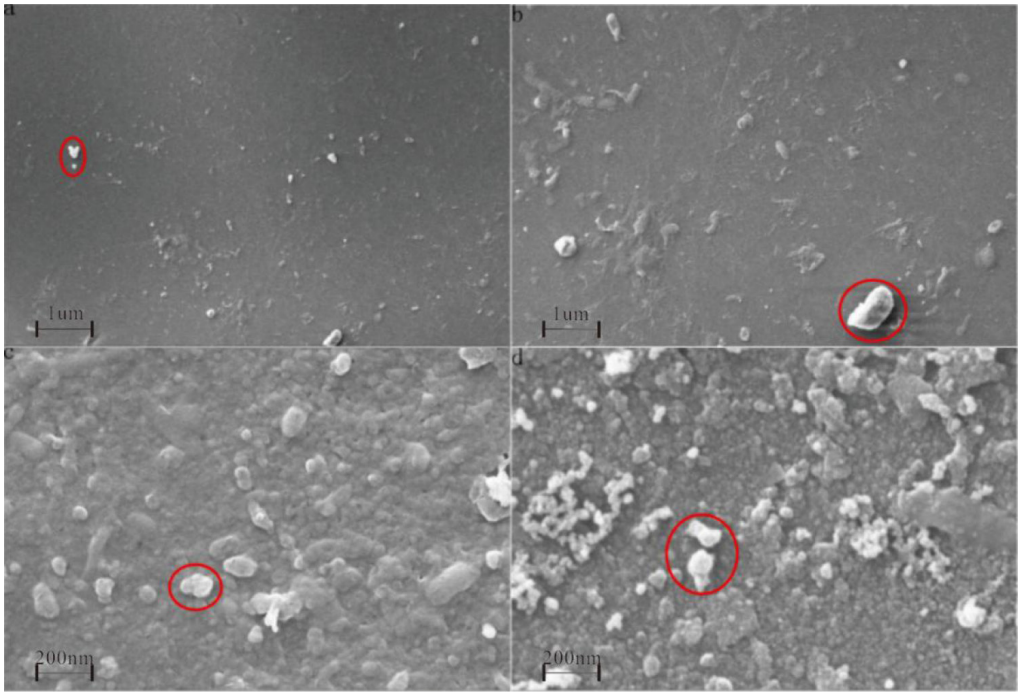

Fig. 5. SEM images of the membrane used for (a) F1, (b) F2, (c) F3 and (d) F4.

ing laye, which had little effect on membrane and resulted in a milder decline of desalination rate.

3.4. Energy consumption

3.4.1. Evaluation of current efficiency

Fig. 6 shows the typical current variations for the four cells on day 1, 5, 10 and 15, respectively. The current graphs for F1 showed the same pattern during the whole operation, in which the current presented a rapid decreasing trend from 150 to 4 mA in the absorption process and then changed from –148 to –5 mA in the desorption process. Similar trend was also observed in F4 at the beginning of operation process. However, the current curve for F4 in the later period was quite different. It was found that the initial operating current in absorption process gradually decreased and this decrement became significant at later period, showing that fouling caused an increment in membrane resistance and thus resulted in a decrement in the initial current. Current efficiency was further compared to investigate the effect of fouling on MCDI performance. The cell for F1 operation exhibited the highest efficiency of 68.6% and kept relatively stable during the whole period. Compared to the slight decline in efficiency of F2 (62.3%), a more pronounced reduction was noticed for F3–F4 and-current efficiency decreased rapidly to 52.4% and 36.1%, respectively. It was due to the fact that, when the feed contained NaCl and BSA, the current was used to absorb NaCl and BSA aggregates which led to a decrement in current efficiency [25], and this decrement was more serious with BSA concentration increasing.

3.4.2. Evaluation of specific energy consumption

Fig. 7 shows the energy consumption of MCDI in the absorption process with different feed solutions, in which the energy consumption ascended with the increment of BSA concentration. When the MCDI cell was fed with F1, the energy consumption kept relatively constant with averaged 1.52 W·h/g during the whole period, which was mainly attributed to the stable quality of salt ions adsorbed on the electrode. In the case of F2, slight increment in energy consumption was observed and the value gradually increased to 1.84 W·h/g within 15 d. Comparatively, the energy consumption presented a faster increasing rate and there were significant differences in variation process for F3 and F4 treatment, which could also be divided into three stages, including the initial stage, high growth stage and stable stage that consistent with the fouling process. Specifically, the cell fed with F3 slightly increased to 1.67 W·h/g within 4 d, then quickly increased to 2.52 W·h/g in the following 8 d, and lastly tended to be stable with the final value of 2.78 W·h/g. For F4, a similar increasing trend

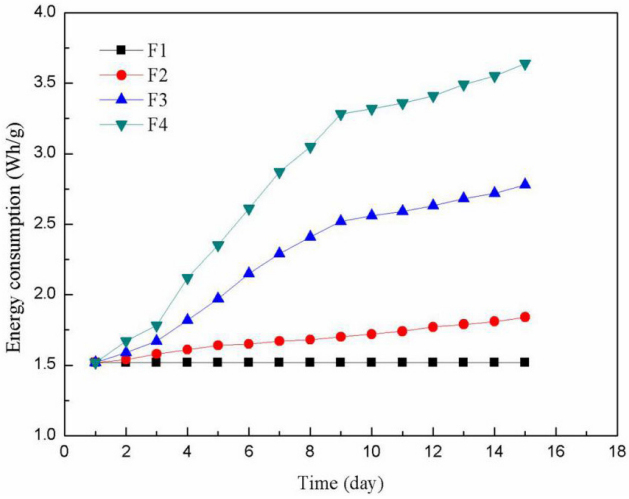

Fig. 7. Variations of energy consumption as processing different BSA concentrations.

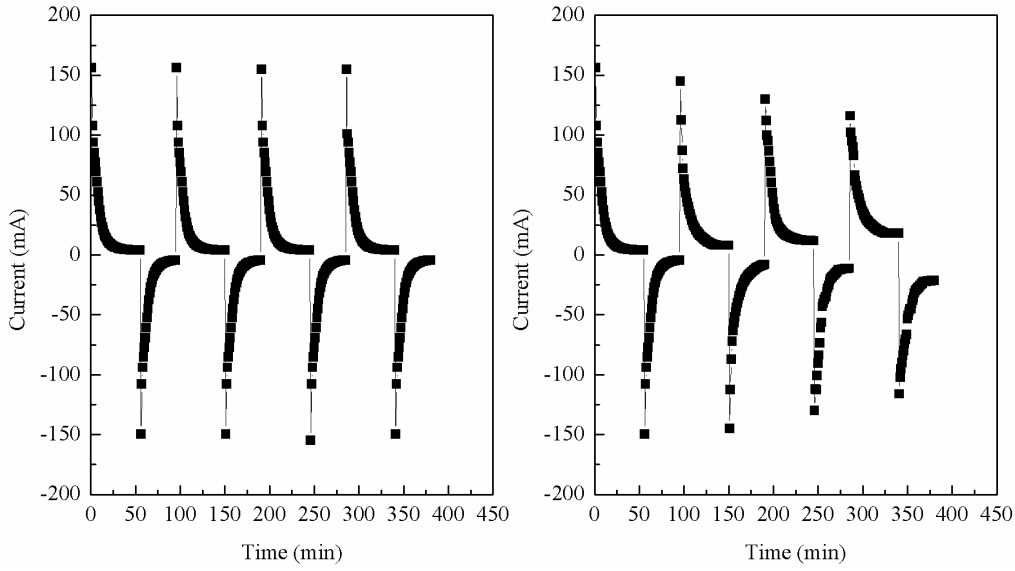

Fig. 6. Current variations for (a) solution F1 and (b) solution F4 in MCDI operation.

in energy consumption was obtained while with more significant increment. The main factor for the consumption of additional energy was the accumulation of proteins on the membrane surface and the plugging of membrane pores, which increased electrical resistance.

3.5. Strategies of membrane cleaning

In this study, the cleaning procedure for ion-exchange membranes included the following stages: rinsing step with DI water and chemical cleaning step, wherein ultrasonic cleaning was applied in these steps. Specifically, the chemical cleaning step included acid cleaning and alkaline cleaning, and the cleaning agents were citric acid and sodium hydroxide, respectively, and the cleaning time lasted for 90 min for each cleaning step. The desalination recovery was evaluated after each cleaning step and the results are presented in Fig. 8, in which it was obtained that chemical cleaning combined with ultrasonic was much effective in the enhancement of the fouling layer removal and the diminution of the pores plugging, which was due to the collapse of the microbubbles generated by ultrasonic cleaning [26]. For DI water cleaning and acid cleaning, it was beneficial to remove inorganic salts and the desalination slightly increased to 68.3%, 49.1% and 31.5%, respectively. Comparatively, the recovery value was greatly improved for the last cleaning step of alkaline cleaning with the value of 98.0%, 76.7% and 60.6%, indicating that the alkaline cleaning was more effective in removing dissolved organic materials which deposited on the membrane surface and membrane pores.

3.6. Further research directions

MCDI technology was a promising desalination technology, while further study on the membrane fouling was necessary before realizing the economic feasibility. Relative study about the effect of foulants on MCDI desalination performance was quite scarce and to the best of our knowledge, Kim et al. [27] was the only research group who had studied. Membrane fouling was a combined result of interaction between multiple factors and components, suggesting that the fouling process in MCDI should be a dynamic and complex process. The aim of this study was to lead attention to membrane fouling in MCDI process and provide some reference research directions. Moreover, this study mainly investigated the effect of surface fouling on MCDI performance and further study about electrode fouling would be conducted in the next.

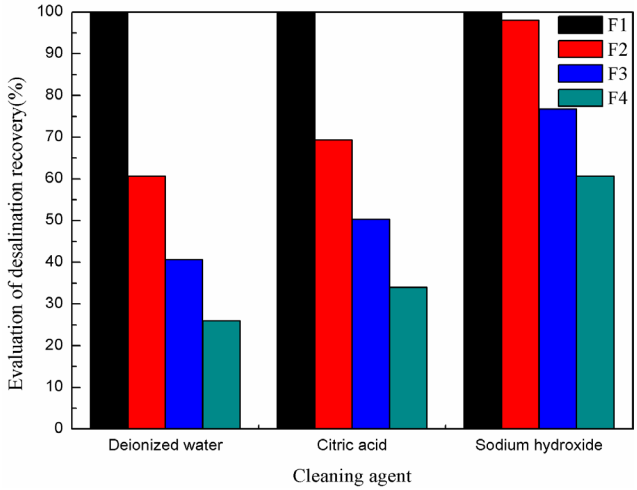

Fig. 8. Evaluation of desalination recovery.

4. Conclusions

In this study, the effect of BSA on MCDI performance was investigated which was characterized by the desalination rate, energy consumption and membrane properties, and the following conclusions were obtained:

Severe decline in the desalination rate could be found when the feed contained BSA and the value for F2, F3 F4 decreased from 48.1% to 23.1%, 12.1%, 4.3%, respectively. As BSA concentration was increased, it was observed that there was a more rapid decreasing trend in the desalination performance, indicating the increasing degree of fouling phenomenon caused by the increment in BSA attachment onto membrane surface.

The adverse effects were also reflected in the deterioration of membrane properties, including the increment in electrical resistance, and decrement in ion exchange capacity, water content and transport number.

For the solution in the presence of BSA, additional energy was consumed by BSA to move towards membrane and be absorbed on the surface, and hence the energy consumption increased correspondingly.

Additionally, for the feed with the presence of BSA, additional energy was consumed by BSA to move towards membrane and be absorbed on the surface, and hence the energy consumption increased correspondingly.

Furthermore, cleaning strategy for fouled membrane was evaluated by desalination recovery. Results showed that alkaline cleaning combined with ultrasonic could significantly recovered the desalination, and the discrepancy in cleaning effects indicated the major fouling materials.

Acknowledgement

This study was mainly financially supported by National Natural Science Fund of China (grant number: 51508153), Natural Science Fund of Jiangsu (grant number: BK20150813), Fundamental Research Funds for the Central Universities (2018B15014) and A Project Funded by the Priority Academic Program Development of Jiangsu Higher Education Institutions.

References

[1] F.A. AlMarzooqi, A.A. Al Ghaferi, I. Saadat, N. Hilal, Application of capacitive deionisation in water desalination: A review, Desalination, 342 (2014) 3–15.
[2] Y. Sun, Z. Chen, G. Wu, Q. Wu, F. Zhang, Z. Niu, H.-Y. Hu, Characteristics of water quality of municipal wastewater treatment plants in China: implications for resources utilization and management, J. Clean. Prod., 131 (2016) 1–9.

[3] R. Zhao, P.M. Biesheuvel, A.V.D. Wal, Energy consumption and constant current operation in membrane capacitive deionization, Energ. Environ. Sci, 5 (2012) 9520–9527.
[4] P. Xu, J.E. Drewes, D. Heil, G. Wang, Treatment of brackish produced water using carbon aerogel-based capacitive deionization technology,Water. Res., 42 (2008) 2605–2617.
[5] H. Li, L. Zou, Ion-exchange membrane capacitive deionization: A new strategy for brackish water desalination, Desalination, 275 (2011) 62–66.
[6] J.K. Lee, E.K. Ye, J. Kim, S. Chung, D. Ji, J. Lee, Comparable mono and bipolar connection of capacitive deionization stack in NaCl treatment, J. Ind. Eng. Chem., 18 (2012) 763–766.
[7] Y.J. Kim, J.H. Choi, Improvement of desalination efficiency in capacitive deionization using a carbon electrode coated with an ion-exchange polymer, Water. Res., 44 (2010) 990–996.
[8] H. Li, C. Nie, L. Pan, Z. Sun, The study of membrane capacitive deionization from charge efficiency, Desal. Water. Treat., 42 (2012) 210–215.
[9] C. Huyskens, J. Helsen, W.J. Groot, A.B. de Haan, Cost evaluation of large-scale membrane capacitive deionization for biomass hydrolysate desalination, Sep. Purif. Technol., 146 (2015) 294–300.
[10] E. Belashova, S. Mikhaylin, N. Pismenskaya, V. Nikonenko, L. Bazinet, Impact of cation-exchange membrane scaling nature on the electrochemical characteristics of membrane system, Sep. Purif. Technol., 189 (2017) 441–448.
[11] W.S. Ang, M. Elimelech, Protein (BSA) fouling of reverse osmosis membranes: Implications for wastewater reclamation, J. Membr. Sci., 296 (2007) 83–92.
[12] H.-J. Lee, D.H. Kim, J. Cho, S.-H. Moon, Characterization of anion exchange membranes with natural organic matter (NOM) during electrodialysis, Desalination, 151 (2002) 43–52.
[13] G. Naidu, S. Jeong, S.-J. Kim, I.S. Kim, S. Vigneswaran, Organic fouling behavior in direct contact membrane distillation, Desalination, 347 (2014) 230–239.
[14] N. Tanaka, M. Nagase, M. Higa,Organic fouling behavior of commercially available hydrocarbon-based anion-exchange membranes by various organic-fouling substances, Desalination, 296 (2012) 81–86.
[15] W. Wang, R. Fu, Z. Liu, H. Wang, Low-resistance anti-fouling ion exchange membranes fouled by organic foulants in electrodialysis, Desalination, 417 (2017) 1–8.
[16] M. Pontié, S. Ben Rejeb, J. Legrand, Anti-microbial approach onto cationic-exchange membranes, Sep. Purif. Technol., 101 (2012) 91–97.
[17] N. Yoshida, A.T. Ishisaki, Watakabe, M. Yoshitake, Characterization of Flemion1 membranes for PEFC, Electrochim. Acta, 43 (1998) 3749–3754.
[18] M.K. Cho, H.-Y. Park, S. Choe, S.J. Yoo, J.Y. Kim, H.-J. Kim, D. Henkensmeier, S.Y. Lee, Y.-E. Sung, H.S. Park, J.H. Jang, Factors in electrode fabrication for performance enhancement of anion exchange membrane water electrolysis, J. Power Sources, 347 (2017) 283–290.
[19] R.E. Brown, K.L. Jarvis, K.J. Hyland, Protein measurement using bicinchoninic acid: elimination of interfering substances, Anal. Biochem., 180 (1989) 136–139.
[20] K.-J. Hwang, P.-Y. Sz, Membrane fouling mechanism and concentration effect in cross-flow microfiltration of BSA/dextran mixtures, Chem. Eng. J., 166 (2011) 669–677.
[21] A. Bottino, G. Capannelli, O. Monticelli, P. Piaggio, Poly(vinylidene fluoride) with improved functionalization for membrane production, J. Membr. Sci., (2000) 23–29.
[22] I. Sharma, S.K. Pattanayek,Effect of surface energy of solid surfaces on the micro- and macroscopic properties of adsorbed BSA and lysozyme, Biophys. Chem., 226 (2017) 14–22.
[23] S.T. Kelly, A.L. Zydney, Mechanisms for BSA fouling during microfiltration, J. Membr. Sci., 107 (1995) 115–127.
[24] K. Nakamura, K. Matsumoto, Properties of protein adsorption onto pore surface during microfiltration: Effects of solution environment and membrane hydrophobicity, J. Membr. Sci., 280 (2006) 363–374.
[25] Y. Zhao, Y. Wang, R. Wang, Y. Wu, S. Xu, J. Wang, Performance comparison and energy consumption analysis of capacitive deionization and membrane capacitive deionization processes, Desalination, 324 (2013) 127–133.
[26] M.J. Luján-Facundo, J.A. Mendoza-Roca, B. Cuartas-Uribe, S. Álvarez-Blanco, Ultrasonic cleaning of ultrafiltration membranes fouled with BSA solution, Sep. Purif. Technol., 120 (2013) 275–281.
[27] Y.J. Kim, H. Jin, W. Bae, J.H. Choi, Desalination of brackish water containing oil compound by capacitive deionization process, Desalination, 253 (2010) 119–123.